Characterization of thermal flow sensors for air flow measurements in transport containers

Safir Issa[1,2], Walter Lang[1,2]

[1]IMSAS (Institute for Microsensors, Actuators and Systems), Microsystems Center Bremen (MCB), University of Bremen, Otto-Hahn-Allee, Bld. NW1, D-28359 Bremen, Germany

[2]IGS (International Graduate School for Dynamics in Logistics), University of Bremen, c/o BIBA Hochschulring 20, D-28359 Bremen, Germany;

{sissa, wlang}@imsas.uni-bremen.de

Abstract Air flow measurements inside containers for sensitive and perishable products effectively participate in improving transport processes. Results of such measurements allow taking preventive actions to maintain the desired temperature during transport trips. Consequently, we can optimize the quality of transported goods and reduce their losses. Thermal flow sensors are chosen for these measurements. This paper introduces an overall characterization of these sensors to prove their suitability for the intended objective. The characterization covers the air velocity range from 0 to 5 m/s, which is the expected range in the container. Results show that the characteristic curve is linear for the ultra low flow range and the minimum detectable air velocity is ca. 0.4 mm/s.

Keywords   Characterization, Thermal flow sensors, Transport container

1   Introduction

Nowadays, customers demand a constantly increasing amount of sensitive and perishable products. This fact forces producers and marketers to ensure the arrival of these products to their target consumers in a good quality. In case of fruit and vegetables, temperature is the dominant environmental factor that influences their deterioration. It affects their external shape, quality and shelf life. Temperatures either above or below the optimal range for fresh produce can cause rapid deterioration due to some factors such as freezing, chilling injury or heat injury [1]. Thus maintaining a specific temperature throughout the container during the whole transport process is an essential matter to keep product's quality and to reduce its losses. However, this purpose is very difficult to achieve, due to the fact that air

conditioning system should provide homogeneous distribution of air flow inside the container, which in reality is not possible. Additionally, the internal production of heat and moisture generated by fruit and vegetables are supplementary parameters that affect the temperature profile. Furthermore, the internal geometry of containers participates in the non-uniform distribution of temperature. All equipped pallets and boxes can provide only narrow spaces and holes for air current passages. This crucial role of temperature not only encourages researchers to measure it in real time, but also to predict its values in advance. Such prediction allows taking preventive actions to maintain temperature within the allowable limits. One of the essential methods to predict temperature variations is the air flow measurement. The temperature and its distribution are controlled by air flow pattern [2]. Thus performing air flow measurements will provide a better understanding of convection transport inside the container and will identify the stagnant zones where the air flow is very poor. Temperatures in these zones are surely higher than expected as the air circulation is not able to convect the generated heat. In the next level, the measurement results will help in the optimization of air circulation and the improvement of efficiency of the air conditioning system, to avoid forming stagnant zones and to obtain more homogeneity in temperature distribution.

In the literature there are some reports about studying air flow patterns for the perishable goods transportation. Zou et al. [3] develop a computational fluid dynamics (CFD) modeling system of the airflow patterns and heat transfer inside ventilated packages for fresh food. This research is concerned by food packages and not the whole container. Moureh et al. [2] introduced reports on the numerical and experimental characterization of airflow within a semi-trailer enclosure loaded with pallets in a refrigerated vehicle with and without air ducts. Measurements of air velocities were carried out by a laser Doppler velocimeter in clear regions (above the pallets) and thermal sphere-shaped probes located inside the pallets. The velocimeter is placed outside the vehicle and the measurement is done through a glass window.

The present work is a part of the above referred objective; air flow measurements inside logistic containers by means of thermal flow sensors. It proves the suitability and the capability of the chosen sensors to perform the intended measurements. They are micro sensors developed by IMSAS [4]. This choice is based on the multi measurement requirements in containers. Their very small size enables placing them in different positions in the container i.e. on walls, ceiling, between pallets, inside boxes, etc. Moreover, these sensors are able to send data through wireless network by using RFID technologies, and to be integrated within a sensor network such as presented in [5]. Additionally, they have a fast response time [6].

In this paper, an overall characterization for these sensors is studied. Paragraph 2 describes the measurement setup and the characteristic curves of the sensors. Paragraph 3 focuses on the minimum detectable flow which is investigated by both theoretical calculation and experimental measurements.

2   Measurement setup and characteristic curves

The investigated thermal flow sensors are based on silicon as substrate material; they consist of a heater and two symmetric thermopiles embedded in silicon nitride membrane. The heater is made of tungsten-titanium, whereas the thermopiles are made of a combination of polycrystalline silicon and tungsten-titanium. In case of zero flow, the heat generated by the heater is distributed uniformly to both sides and no difference in temperature is detected by the thermopiles signals. However, in the case of flow, there is a difference in temperature between the two signals, as the air flow convects a part of the generated heat. This difference is related to the value of flow and will be the interesting part for the sensor characterization. Four sensor configurations are considered in this study TS5, TS10, TS20 and TS50. They have the same membrane area of 1 mm^2 and differ in the distance between heater and thermopiles. This distance is 5 µm for TS5 and 50 µm for TS50.

Two flow ranges are studied to separate the linear part of the characteristic curve from the whole curve. The ultra-low flow is from 0 to 10 SCCM (Standard Cubic Centimeter per Minute) and the low flow is until 1000 SCCM. They cover the probable air velocity values inside the container from 0 to 5 m/s. In the characterization setup, three mass flow controllers with maximum capacities: 20, 200 and 1000 SCCM from MKS Company are used. They are connected through pipes to an air supply source from one side and to the sensor air channel from the other side as shown in Fig. 1. These controllers are driven by a control unit MKS through a LabVIEW program. According to this program several mass flow controllers are chosen with an adjustable flow steps. The sensor is operated in constant power mode and the two thermopile's signals are extracted by NI (National Instruments) data acquisition device. The data of sensor's outputs with the related flow values are stored in a PC.
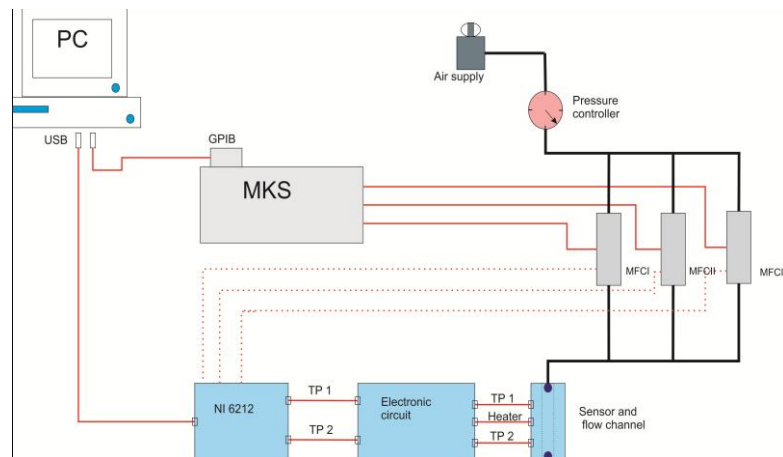
Fig. 1. . Measurement setup for characterization of thermal flow sensors

Firstly, the ultra-low-flow is discussed. In this case only one MKS mass flow controller is used with maximum capacity of 20 SCCM. By analyzing the extracted data, we calculate the output voltage difference which is the difference between the two thermopile signals as a function of air flow. The resulting curve is called the characteristic curve. We compare then the curves of the four sensor configurations TS5, TS10, TS20 and TS50. Fig.2 shows this comparison, these curves are all linear as they are in a good agreement with the linear fitting. The R-squared values are all in the range of 0.999. This fact indicates that the fitting degree is very high. We can notice that the sensor sensitivity increases with the distance between the heater and the thermopiles. This gives advantages to select TS50 sensor for future measurements in containers. It is important to mention that these sensors have a small zero offset due to a slight difference between the up- and downstream thermopiles. When the two thermopiles are perfectly identical, they give the same signal at zero flow, else a small difference between the two signals is noticed, which cause the zero offset. The zero offset values are taken into consideration to allow all curves to start from the same point for comparison.
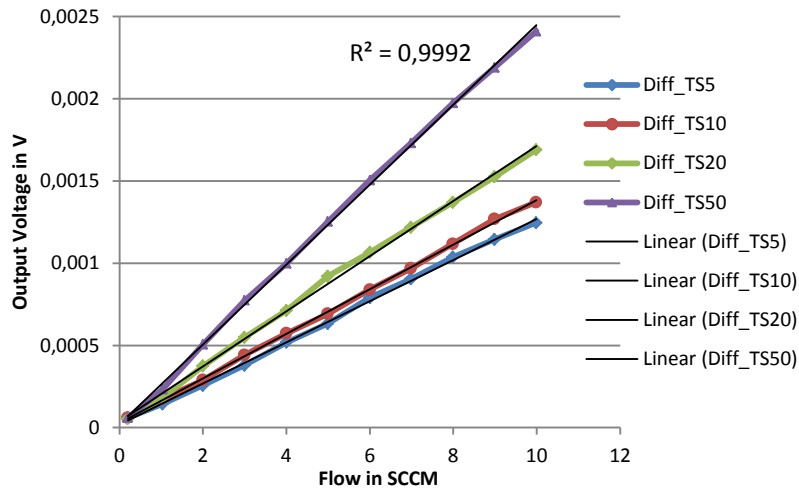
Fig. 2. Thermopiles output voltage difference as function of flow with the linear fitting for the four sensors configurations TS5, TS10, TS20 and TS50

Secondly, the low-flow case is presented. Here we use 3 mass flow controllers, with maximum capacities 20, 200 and 1000 SCCM. The characteristic curves for the four sensor configurations are extracted as in the ultra-low flow case. The output voltage difference starts to increase linearly with the air velocity untill a certain limit and then continues its increase but in non linear way as in Fig. 3. The function model that specifies the relationship between air velocity and voltage difference is:

$$\Delta E = a\, e^{bu} + c\, e^{du}$$

where ∆E is the output voltage difference of the sensor; u is the air velocity; a,b,c and d are constants to be determined for each sensor configuration. We use the MATLAB based function fminsearchbnd to find the suitable fits. Substituting experimental measurement results in the model formula enables estimating the best values of the constants for the best fit. Fig. 3 shows the characteristic curves with their fits of the four sensor configurations as function of air velocity. Moreover, Table 1 depicts the constant values of a,b,c and d in addition to the R- squared values which are very close to 1. These results ensure the suitability of the fits.
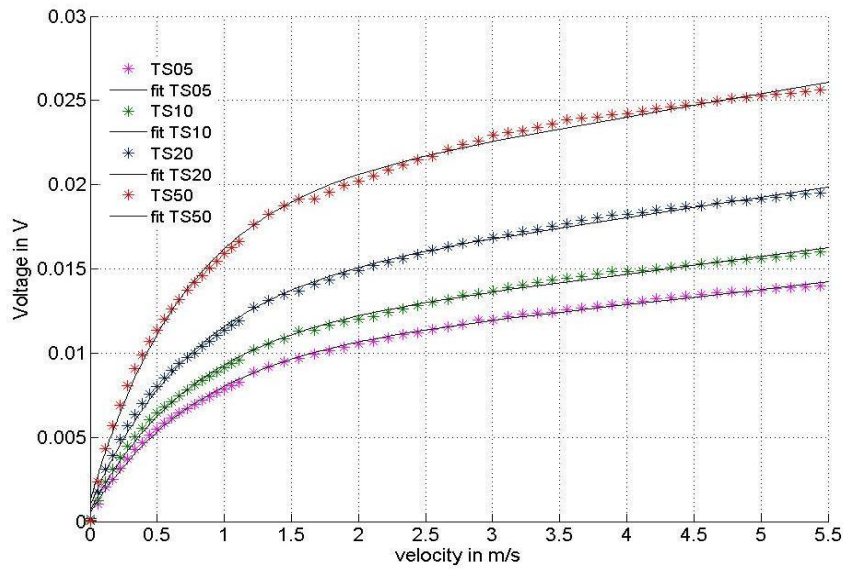
Fig. 3. Characteristic curves with fits of the four sensor configurations: TS5, TS10, TS20 and TS50. Dots are the experimental results and the lines are the fits.

Table 1. Values of constants for the fitting curves and the R-squared values

	a	b	c	d	R_seq
TS05	0.01	0.0638	0.0095	1.2735	0.9987
TS10	0.0114	0.0647	0.0107	1.33	0.9982
TS20	0.0142	0.0616	0.0131	1.3284	0.9981
TS50	0.0194	0.0539	0.0181	1.4459	0.9973

3   Minimum detectable air velocity

The minimum detectable flow is a parameter characterizes flow sensors. It becomes very important when these sensors are used for very low-flow applications. This parameter is basically influenced by natural convection and thermopile noises. Firstly, the natural convection is a mechanism in which the fluid motion is generated by density differences in the fluid due to temperature gradients [7]. Air surrounding the sensor heater receives heat, becomes less dense and rises. The surrounding, cooler air then moves to replace it. This cooler air is then heated and the process continues, forming convection current. Natural convection air velocities are very small and can be neglected in many cases, especially when there is a (forced) air flow through the sensor's channel. Secondly, the thermopile noises are basically the temperature noise and the thermal noise. The temperature noise is caused by temperature fluctuations in the surrounding atmosphere. We assume that this noise has negligible effect on our calculations. The thermal noise or the Johnson noise is an electrical noise source caused by random motion of electrical charges in the material. The Johnson noise is determined by [8]:

$$V_{noise} = \sqrt{4 \cdot k_B \cdot T_{ext} \cdot R_e \cdot \Delta f}$$

where k_B is the Boltzmann's constant; T_{ext} is the external temperature; R_e is the electrical serial resistance and Δf is the frequency bandwidth.

With $k_B = 1.38066 \times 10^{-23}$ JK^{-1}; $T_{ext} = 323$ K; $R_e = 200$ KΩ; $\Delta f = 1000$ Hz. The noise is then 1.89 µV.

To identify the experimental noise level, the sensor output signals are extracted in the zero flow case. The signals are registered through a LabVIEW program for 1000 samples with time interval of 5 s. Fig. 4 shows the sensor's output voltage difference as function of time.
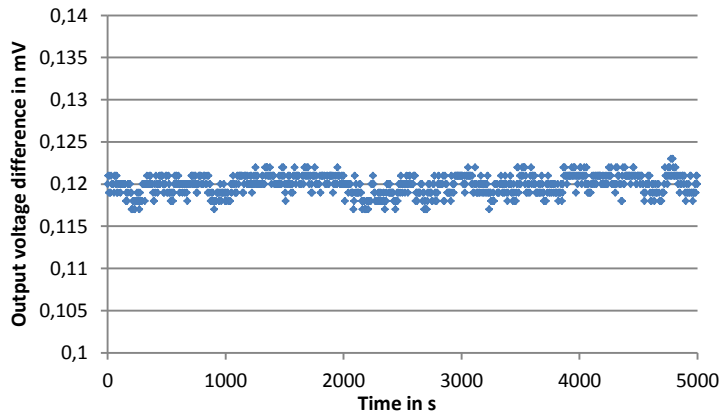
Fig. 4. Sensor output signal (thermopiles voltage difference) vs. time in the zero flow case

We analyze statistically the results to calculate the arithmetic mean and the uncertainty. The arithmetic mean value is 0.1198 mV, assumed to be the zero offset of the sensor. The expanded uncertainty of a measurement U is given by [9]:

$$U = k \cdot u_c$$

where k is the coverage factor *and* u_c is the combined uncertainty. Assuming that the sample' values follow a Normal distribution function, then for a level of confidence 95%, the coverage factor k equals 2 [8]. u_c combines all uncertainty components. We assume that the statistically-evaluated components are the dominant ones. Then u_c is restricted to the standard deviation of the sample values. The standard deviation of the results is 0.0011 mV and, the corresponding measurement expanded uncertainty is 2.3 µV. Comparing this value with the thermal noise which is 1.89 µV enables estimating the effect of the other parameters on sensor output signal, in the stagnant flow case. To calculate the minimum detectable velocity, we still need the sensor's sensitivity value. It is defined as the derivative of the output voltage difference with respect to the flow velocity at a zero flow as in the following equation [10]:

$$S = \left.\frac{\partial V_{diff}}{\partial u}\right|_{u=0}$$

In other words, sensitivity is the slope of the sensor's characteristic curve. For example, sensitivity of TS50 is 0.044 V/(m/s), the minimum detectable velocity is estimated then to be: 2.3 µV/0.044 V/(m/s) = 0.05 mm/s. This value is recognized by the sensor, not as noise.

Experimentally, different methods are investigated to determine the minimum detectable velocity value. The first one is done by using mass flow controller of maximum capacity of 20 SCCM. According to its specifications, the control range is from 2% to 100% of full scale. The equivalent velocity range is from 2.22 to 111 mm/s as the air-channel area is 1.5×2 mm². All measurements performed by this controller show that velocities lower than 1 mm/s cannot be identified. This value is 20 times higher than the theoretical estimated value. Therefore, a physical method is established to generate smaller flow rates. This method is shown in Fig. 5.
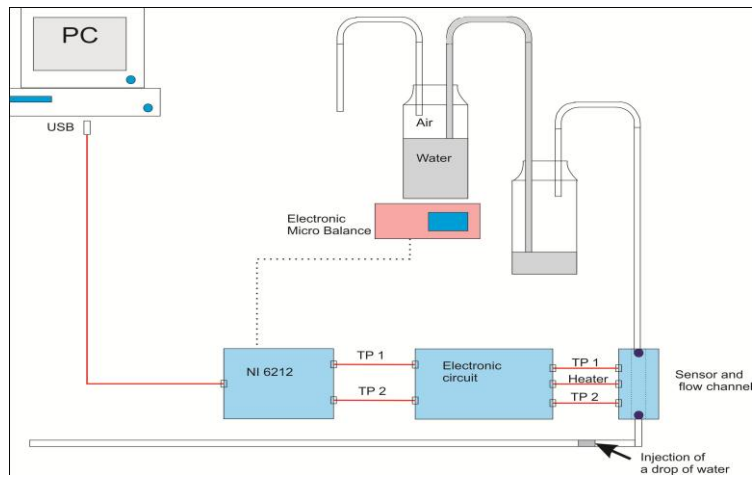
Fig. 5. Setup for generating very small flow rates. The flow is identified by two methods: first by measuring the water flow rate between two closed bottles. Second method is by injection a drop of water in the outlet pipe of the sensor and estimating its velocity.

We initiate a water flow between two perfectly closed bottles, placed in different height positions. This forces an equivalent air flow from the second bottle to be created. The air flow is guided through a pipe to the sensor air-channel

As initial condition, the first bottle is half full of water, and the second one is empty. Then we consider three different cases regarding the height positions of the two bottles. In such a way their height differences are: large, moderate and small respectively. In the first two cases, the first bottle is discharged completely into the second one, but of different speeds. Whereas in the third case, water starts to flow slowly between the two bottles until equilibrium is reached. This can happen when the two bottles have the same water level. Fig.6. compares the water mass flow vs. time for the three cases. In the first position, the flow decreases in linear way from 0.15 to 0.09 g/s. In the second position, the flow decreases slowly from ca. 0.08 to 0.015 g/s. In the last case, the velocity has a parabolic curve; it decreases very slowly toward zero. We are particularly interested in the latter case.
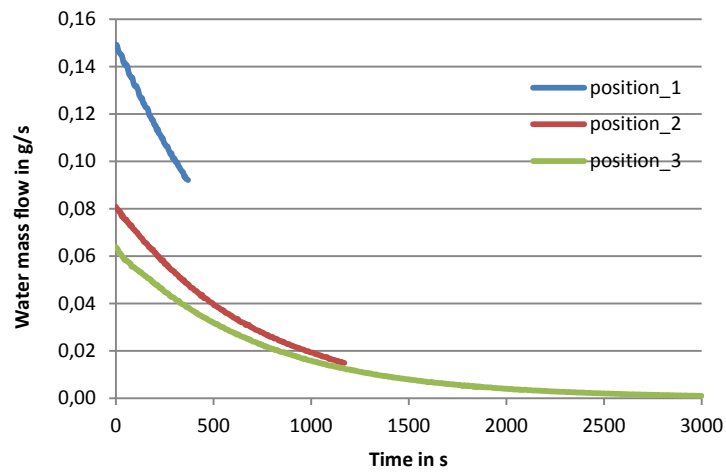
Fig. 6. Comparison of water mass flow between two bottles placed in three different positions regarding their height difference. The height differences are large, moderate and small respectively.

The associated LabVIEW program extracts the sensor output synchronized with the balance reading. We calculate the equivalent induced air flow and then the air velocity through the sensor air channel. From these data the curve of the sensor output is plotted vs. the air velocity as in Fig. 7. The sensor is capable to detect very small velocities. However, sensor output fluctuations increase when flow is in the vicinity of zero. This is due to several reasons: sensor noise, balance reading changes and also air humidity. Nevertheless, by this method the sensor can detect velocities less than 0.4 mm/s with uncertainty of sensor output signal of about +/- 0.02 mV. This uncertainty value decreases significantly with the increase of air velocity.
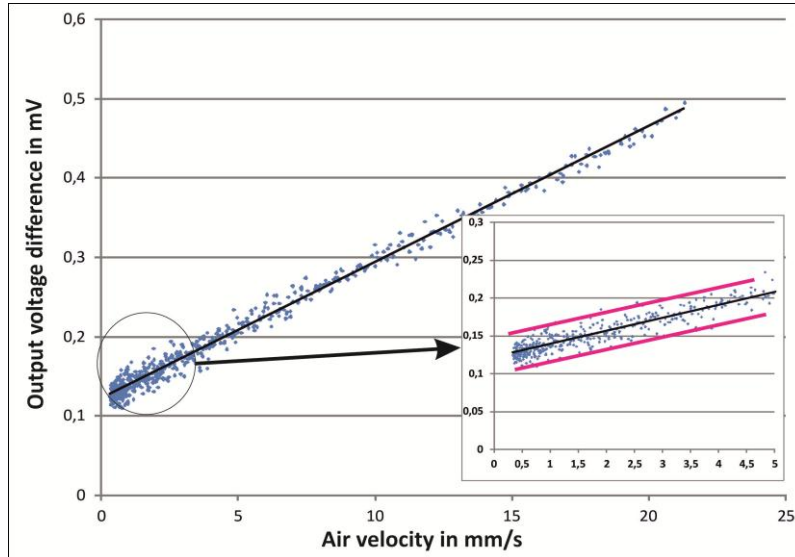
Fig. 7. Sensor output voltage difference as function of air velocity in the ultra low flow range.

Finally, a third method is examined, by using the same setup shown in Fig. 5. The air flow in the outlet of the air channel is guided through a long straight pipe. A drop of water is injected into this pipe which will be pushed by the air flow. Thus, knowing its speed enables determining air velocity through the air channel. This can be done easily by measuring the distance traveled by the water drop within short time steps. By this method we can achieve very low speed values, less than 0.1 mm/s, but unfortunately the sensor output signals for such values are in the noise level. For this reason we adapt the result obtained by the second method.

4   Conclusion

In this study an overall characterization of thermal flow sensors is achieved for the ultra low and low flow ranges. Results show that the characteristic curves of different sensor configurations are linear for the range from 0 to 10 SCCM. Minimum detectable velocity is about 0.4 mm/s with sensor output voltage difference uncertainty of ca. 0.02 mV. This uncertainty value decreases significantly as the air velocity increases. As a result, these sensors are capable to perform very precise air flow measurements inside transport containers. They also fulfill the different requirements imposed by the container conditions. Performing these measurements will help improving transport processes by maintaining quality and reducing losses of the transported products.

References

[1] The role of post-harvest management in assuring the quality and safety of horticultural produce. FAO Corporate Document Repository, (2004).

[2] Moureh, J., Tapsoba, S., Derens, E. & Flick, D. Air velocity characteristics within vented pallets loaded in a refrigerated vehicle with and without air ducts. International journal of refrigeration **32**, 220-234 (2009).

[3] Zou, Q., Opara, L. U., & McKibbin, R. A CFD modeling system for airflow and heat transfer in ventilated packaging for fresh foods. Journal of Food Engineering **77**, 1048–1058 (2005).

[4] Buchner, R., Sosna, C., Maiwald, M., Benecke, W. & Lang, W. A high temperature thermopile fabrication process for thermal flow sensors. Sensors and Actuators A: Physical **130-131**, 262-266 (2006).

[5] Jedermann, R., Ruiz-Garcia, L. & Lang, W. Spatial temperature profiling by semi-passive RFID loggers for perishable food transportation. Computers and Electronics in Agriculture **65**, 145-154 (2009).

[6] Issa, S.; Sturm, H.; Lang, W., Modeling of the Response Time of Thermal Flow Sensors. Micromachines **2**, 385-393 (2011).

[7] Incropera, F. P. & DeWitt, D. P. Fundamentals of Heat and Mass Transfer. 5 edn, John Wiley & Sons, (2002).

[8] Johnson, J. B. Thermal Agitation of Electricity in Conductors. Physical Review **32**, 97-109 (1928).

[9] JCGM 100:2008. Evaluation of measurement data – Guide to the expression of uncertainty in measurement. 1st ed. September 2008.

[10] Kaltsas, G. & Nassioppoulou, A. G. Novel C-MOS compatible monolithic silicon gas flow sensor with porous silicon thermal isolation. Sensors and Actuators A: Physical **76**, 133-138 (1999)